

Simulation and Analysis of Methylammonium Lead Iodide ($\text{CH}_3\text{NH}_3\text{PbI}_3$) Perovskite Solar Cell with Au Contact Using SCAPS 1D Simulator

Ali Husainat^{1,*}, Warsame Ali², Penrose Cofie², John Attia², John Fuller²

¹Department of Electrical and Computer Engineering, Prairie View A&M University, Prairie View, USA

²Department of Electrical and Computer Engineering, Faculty of Electrical Engineering, Prairie View A&M University, Prairie View, USA

Email address:

ahusainat1@student.pvamu.edu (A. Husainat), whali@pvamu.edu (W. Ali), pscofie@pvamu.edu (P. Cofie),

joattia@pvamu.edu (J. Attia), jhfuller@pvamu.edu (J. Fuller)

*Corresponding author

To cite this article:

Ali Husainat, Warsame Ali, Penrose Cofie, John Attia, John Fuller. Simulation and Analysis of Methylammonium Lead Iodide ($\text{CH}_3\text{NH}_3\text{PbI}_3$) Perovskite Solar Cell with Au Contact Using SCAPS 1D Simulator. *American Journal of Optics and Photonics*. Vol. 7, No. 2, 2019, pp. 33-40. doi: 10.11648/j.ajop.20190702.12

Received: July 17, 2019; Accepted: August 10, 2019; Published: August 20, 2019

Abstract: Hybrid organic-inorganic perovskite solar cells have attracted the attention of researchers and scientists throughout the world. From 2009, when actual research work began on photovoltaic perovskite applications, a lab power conversion efficiency above 23.3% have been achieved. Whereas, silicon solar cells have only achieved power conversion efficiencies around 17.5% in both residential and commercial applications. A typical perovskite solar cell consists of 6 main layers of different materials: a glass layer, a thin layer of fluorine-doped tin oxide substrate (FTO), an electron transport layer of TiO_2 , a perovskite active layer known as methylammonium lead iodide ($\text{CH}_3\text{NH}_3\text{PbI}_3$), a hole transport layer of Spiro-Ometad, and a gold (Au) electrode. This paper summarizes the research that focused on the selective use of the perovskite solar cell's composite materials, specifically, the Spiro-Ometad layer, the methylammonium lead iodide layer ($\text{CH}_3\text{NH}_3\text{PbI}_3$), and the TiO_2 layer with a variation of the thickness of the perovskite layer. Initial simulation results show a power conversion efficiency of 20.34% when using a gold (Au) electrode. Further research is needed, in which new technology for device fabrication will create homogeneous thin-film layers that will be tested for increased efficiency.

Keywords: Modeling, Simulation, Perovskite Solar Cell, Photovoltaics, Inorganic Materials, Organic Materials

1. Introduction

Until now, the silicon solar cell has an efficiency in the range of 12-17.5% PCE, which lead to an extensive search for a new material with better efficiency. Thus, researchers started looking into hybrid materials for photovoltaic applications. Hybrid photovoltaic technology is an emerging field, compared with inorganic silicon solar cells. Since the 1950s, silicon materials used as the primary material in making solar cells. Hybrid organic-inorganic perovskite solar cells have gained special attention since 2009, with exponential efficiency increases from 3.8% to 23.3% PCE. Perovskite solar cells offer a compelling combination of extremely low-cost, ease of fabrication, and high device performance [1, 2]. The perovskite solar cell

(PSC) has the optical and electrical property to absorb not only the visible light spectrum but also the near-infrared as well.

In contrast, the silicon solar cell can only absorb the visible light spectrum. Furthermore, the perovskite solar cell has passed the 23.0% PCE, which makes it an excellent and more efficient alternative to silicon. In this study, we have used a simulation program called Solar cell capacitance simulator (SCAPS) 1D. To model the perovskite solar cell, we used real experiment data in the simulator to analyze the perovskite solar cell. We have also examined the effect of the absorber layer thickness, doping concentrations, and defects on the performance of the solar cell performance [1].

2. Perovskite Structure

Any material that has a similar crystal structure to the mineral CaTiO_3 (Figure 1 and Figure 2) at a different transition state is called perovskite. The formula ABX_3 represents the perovskite crystal structure (Figure 5), where A is a large organic or inorganic cation, B is a smaller inorganic cation such as (Cu^{2+} , Sn^{2+} , Pb^{2+}) [4, 5], and X_3 is an ion from the halogen group (such as Cl^- , Br^- and I^-) that is able to bond with both cations A and B [1]. There are two

main categories of perovskite crystal structure and can be classified into 1) Haloalkanes perovskite and 2) organic-inorganic halide perovskite. Perovskite materials have excellent optoelectronic behavior, which makes them function well as the absorber layer for photovoltaic application, this is the result of their having high absorption coefficients, making them a more efficient alternative to silicon. Another important characteristic is their ferroelectric behavior, which was discovered half a century ago.

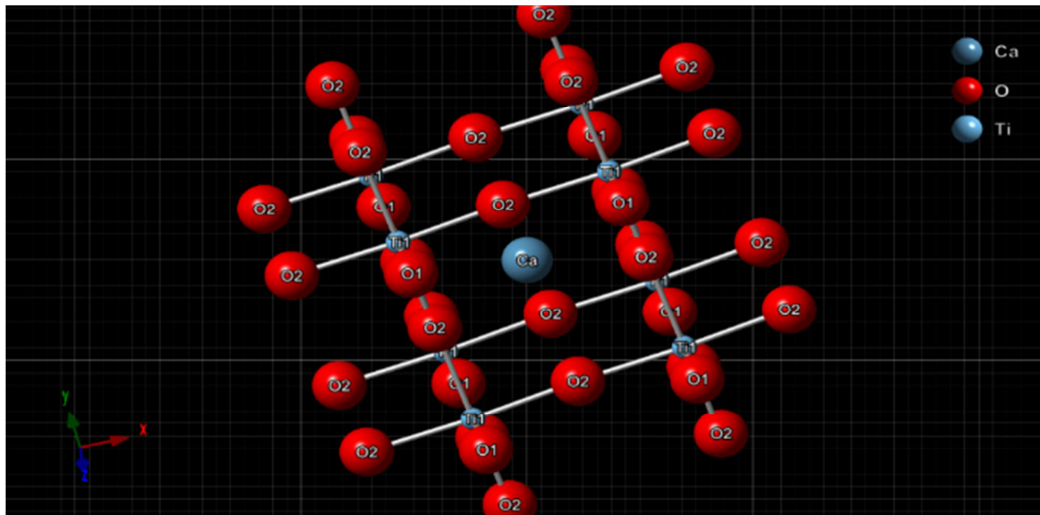


Figure 1. Same as Figure 2, but different view: Many ABX_3 compounds adopt the perovskite structure, with A ions occupying large, 12-fold coordinated sites; B ions are in octahedral coordination by X.

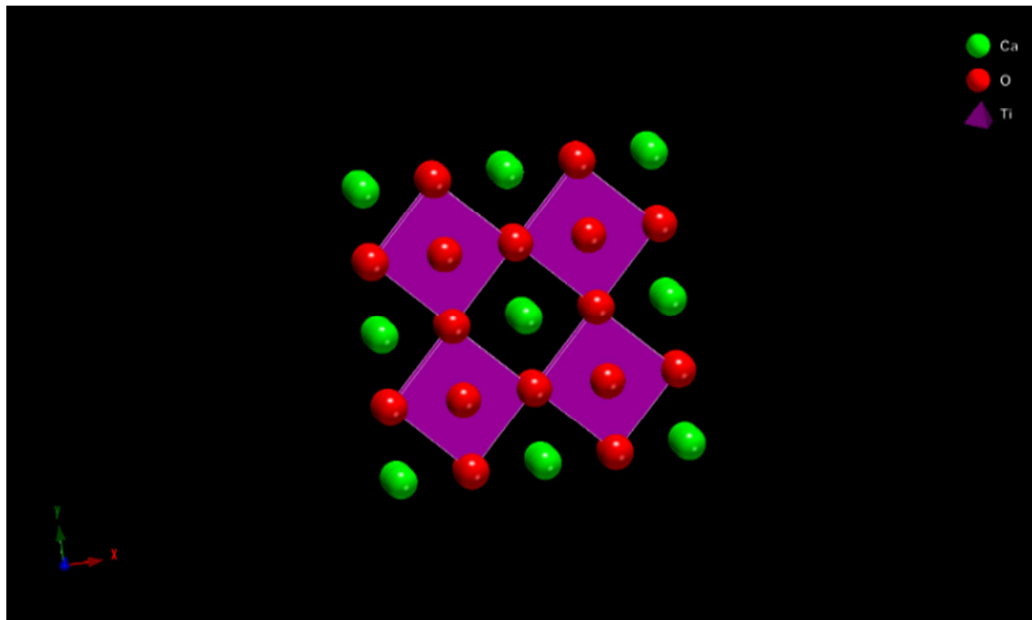


Figure 2. CaTiO_3 Perovskite - TETRAGONAL phase: each titanium atom bonds to six nearest-neighbor oxygen atoms.

Perovskite has a direct bandgap of E_g between 1.3 to 2.2 eV, which gives it the optical properties necessary to harvest and convert near-infrared (NIR) and ultraviolet (UV) light into visible light, which can then be utilized by the perovskite active layer as shown in Figure 3 [5-7].

In the 1990s, scientists discovered that halide perovskite could convert light into electricity. Due to this discovery, the

light-emitting diodes (LED) were made. Perovskite structure has four possible phases, such as 1) α is cubic structure phase occurs at $T > 327$ K. 2) β is a tetragonal structure phase occurs at $T < 327^\circ$ K. 3) γ is orthorhombic structure phase occurs at $T = 160^\circ$ K. 4) δ is a polyhedral phase structure which is a none perovskite phase [8, 9].

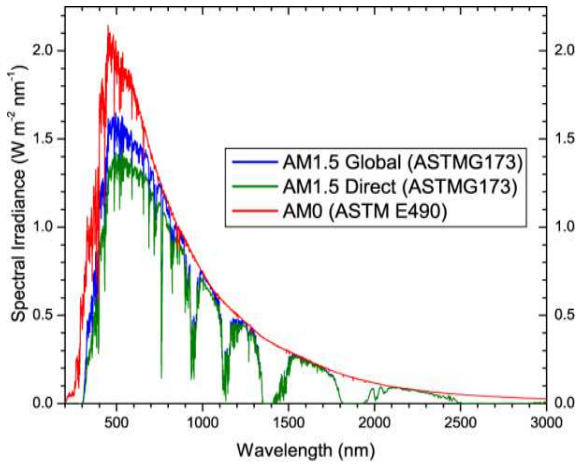


Figure 3. Standard solar spectral (source PVeducation. com).

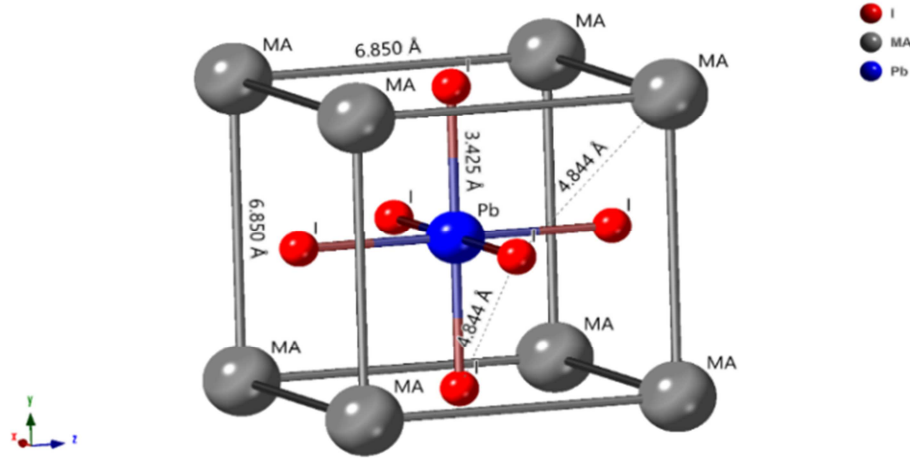


Figure 4. Cubic structure of MAPbI_3 with symmetrical distant between MA-MA, Pb-I atoms.

From 2013 to about mid of 2018, referenced studies [10-12] reported 15.6%, 15.9%, 16.7%, 19.3%, 20.1%, 22.1% and 22.7% PCE respectively. We can see that the PCE of the perovskite solar cell increased very rapidly, as shown in Figure 5.

This comparison makes the perovskite a promising candidate. The primary goal of designing a highly efficient solar cell is to optimize the power conversion efficiency (PCE) to cost ratio. Furthermore, and due to this rapid research and improvement of the perovskite family,

MAPbBr_3 , MAPbCl_3 , and MAPbI_3 . Methylammonium lead iodide (MAPbI_3) is the one that proved to be the best perovskite material due to its excellent electrical and optical properties, low-temperature solution processability, long lifetime, and ferroelectricity. The efficiency of the perovskite solar cell can be further improved through different design techniques to not only the absorber layer but to all other six layers, as shown in Figure 6 [13].

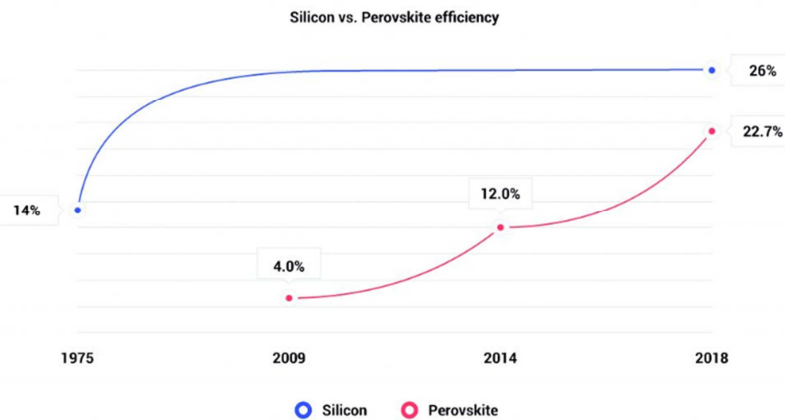


Figure 5. Comparison of the lab efficiencies of Silicon and Perovskite over the years. (source: metSolar. eu).

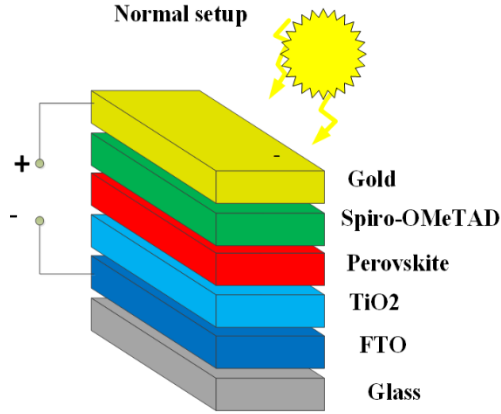


Figure 6. Perovskite solar cell normal setup.

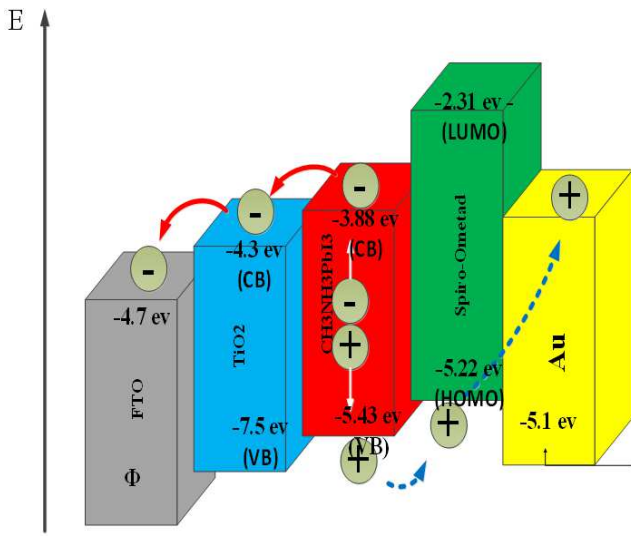


Figure 7. Energy Levels of the Device Layers.

Figure 7 shows the energy levels of the device Layers; it must be in this position for an easy transfer of the electrons and holes through their transport layers to the electrodes.

3. Experimental Details: Simulation and Analysis Approach of Perovskite Solar Cells

Simulation can show the physical operation, the viability of a proposed physical model and is an important way of understanding the device operation, and how the device parameters affect the physical operation and performance of the solar cell devices instantly without the need to wait for long or spend money prior seen a result. There are various simulation models used throughout the photovoltaics technology (AMPS, COMSOL MULTIPHYSICS, GPVDM, SCAPS, SILVACO, and TCAD). In this paper, we use SCAPS 1D simulator to model the perovskite-based solar cells [14] we can define up to 7 semiconductor layers. SCAPS 1D can be used to simulate PSC because it has a very intuitive operation window diversified models for grading,

defects, recombination, and generation. Once all parameters defined, it behaves like a real-life counterpart. The following differential equations in one dimension, are applied:

$$\frac{\partial^2}{\partial x^2} \varphi(x) = \frac{q}{\epsilon} [n(x) - p(x) - N_D^+(x) + N_A^-(x) - p_t(x) + n_t(x)] \quad (2)$$

Poisson's Equation

$$J_{n,p} = nq\mu_n E + qD_n \frac{\partial n}{\partial x} + pq\mu_p E - qD_p \frac{\partial p}{\partial x} \quad (3)$$

Transport equations

$$L_{n,p} = \sqrt{D_{n,p} \tau_{n,p}} \quad (4)$$

Diffusion Length

$$D_{n,p} = \left(\frac{k_B T}{q} \right) \mu_{n,p} \quad (5)$$

Diffusivity

$$\frac{\partial n,p}{\partial t} = \frac{1}{q} \frac{\partial J_n}{\partial x} + (G_n - R_n) + \frac{1}{q} \frac{\partial J_p}{\partial x} + (G_p - R_p) \quad (6)$$

Continuity equation

$$V_{OC} = \frac{n k_B T}{q} \left[\ln \left(\frac{I_L}{I_0} + 1 \right) \right] \quad (7)$$

Where φ : is the electrostatic potential, q is an elementary charge, ϵ is the permittivity, n is the density of free electron, p is the density of free hole, N_D^+ is the ionized donor (doping density), N_A^- is the ionized acceptor (doping density), p_t is the trapped hole density, n_t is the electron trapped density, L_n, p is the diffusion length of electron and holes, $D_{n,p}$ is the electron, hole Diffusivity, μ_n is the electron mobility, τ_n is the electron lifetime, n, p is the electron/hole concentration, E is the electric field, $\frac{\partial n,p}{\partial x}$ is the concentration gradient for the electrons/holes, $G_{n,p}$ is the optical generation rate, $R_{n,p}$ is the recombination rate [15, 16], V_{oc} is the open-circuit voltage, n is the ideality factor, $k_B T/q$ is the thermal voltage, I_L is the solar light generated current, and I_0 is the reverse saturation current.

PSC used in the simulation is an n-i-p structure laid between the n-type semiconductor Titanium Oxide (TiO_2) as an Electron Transport Layer (ETL) and p-type Spiro-OMeTAD as a Hole Transport Layer (HTL). A SnO_2 : F as Fluorine doped Tin Oxide (FTO) is the transparent conductive oxide (TCO), and Au (Gold) as conductor Figure 6 [17, 18]. Solar Cell Capacitance Simulator (SCAPS) is used to simulate PSCs. SCAPS -1D is one of the most widely used device simulators in inorganic solar cells. The simulator uses the three main differential equations 1) Poisson's equation, 2) transport equation, and 3) continuity equation, which is developed by a group of researchers at the University of Gent, Belgium.

4. Photovoltaic Characteristics Used for Device Modeling

In order to study the PSC, SCAPS-1D simulator used Figure 8 and Figure 9 show the input panel to start defining the solar cell different layers. Figure 6 shows PSC structure with different layers such as the contact layer is gold (Au) with a work function of 5.1eV, Spiro-OMeTAD as Hole Transport Layer (HTL) and a p-type with total defect density N_t of $1 \times 10^{15} \text{ cm}^{-3}$. The active layer CH₃NH₃PbI₃ or called the absorber layer, which is the heart of the device [19, 20]. It

is an n-type material, the density set $9 \times 10^{20} \text{ cm}^{-3}$, and the energetic distribution is Gaussian type, which has a characteristic energy value of 0.1 eV and capture cross-section for the electrons and holes are $2 \times 10^{-14} \text{ cm}^2$ and a defect density of $8.5 \times 10^{13} \text{ cm}^{-3}$, which give a carrier diffusion length for electrons and holes of $5.8 \times 10^{-1} \mu\text{m}$. The Electron Transport Layer (ETL) is an n-type with total defect density N_t of $1 \times 10^{15} \text{ cm}^{-3}$. The simulations were performed under the Standard Test Condition (STC) AM1.5G, 1000 W/m², and T=300 K.

Table 1. Photovoltaic characteristics of PSC used in the simulation.

Characteristics	SnO ₂ : F	TiO ₂	CH ₃ NH ₃ PbI ₃	Spiro-OMeTAD
Thickness (nm)	500	100	50-600	300
bandgap (eV) E_g	3.5	3.2	1.55	2.9
electron affinity (eV) χ	4	4.26	3.9	2.2
dielectric permittivity ϵ_r	9	38-108	30	3
CB effective density of states (1/cm ³)	2.20×10^{17}	2.00×10^{18}	2.20×10^{18}	2.50×10^{18}
VB effective density of states (1/cm ³)	2.20×10^{16}	1.80×10^{19}	1.00×10^{18}	1.80×10^{19}
electron thermal velocity (cm/s)	1×10^7	1×10^7	1×10^7	1×10^7
hole thermal velocity (cm/s)	1×10^7	1×10^7	1×10^7	1×10^7
electron mobility (cm ² /Vs)	20	2×10^4	2.20	2.00×10^{-04}
hole mobility (cm ² /Vs)	10	1×10^3	2.2	2.00×10^{-04}
shallow uniform donor density ND (1/cm ³)	1×10^{15}	6×10^{19}	9×10^{20}	0
shallow uniform acceptor density NA (1/cm ³)	0	0	0	1×10^{22}
N_t Total (cm ⁻³)	1×10^{15}	1×10^{15}	8.50×10^{13}	1×10^{15}
Contacts (Au)				
Work function (5.1 eV)				

Figure 8 shows the SCAPS-1D Solar definition panel as it consists of 7 layers that can be defined with different materials and parameters, as seen in figure 9.

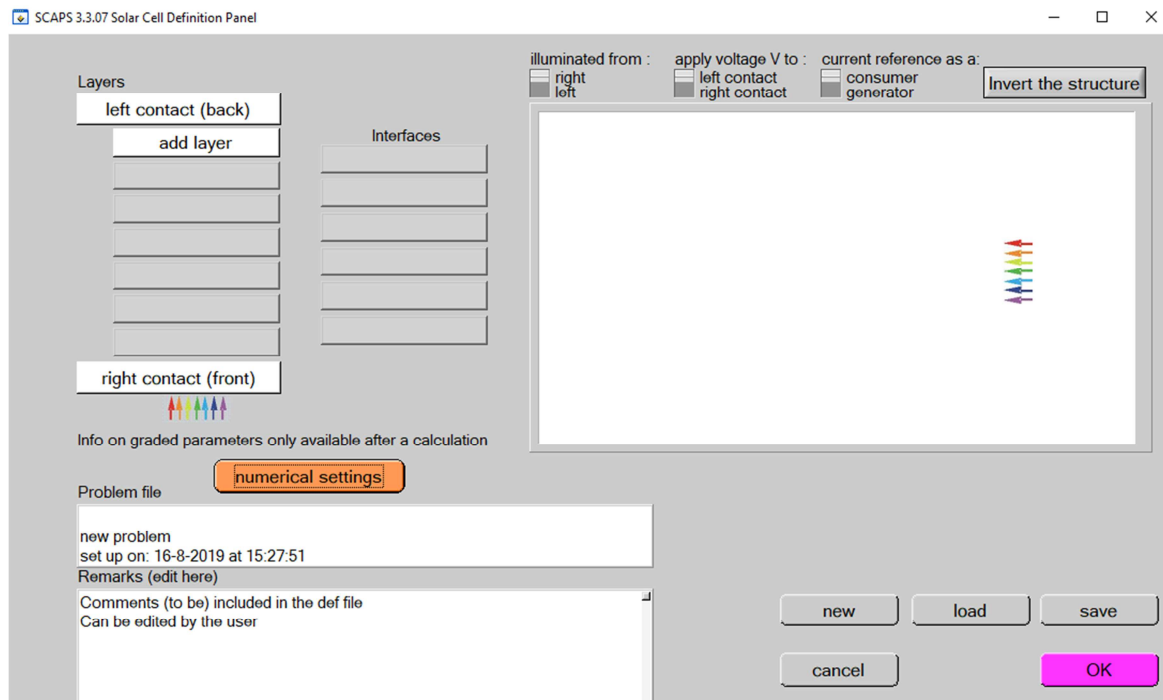


Figure 8. SCAPS-1D definition panel.

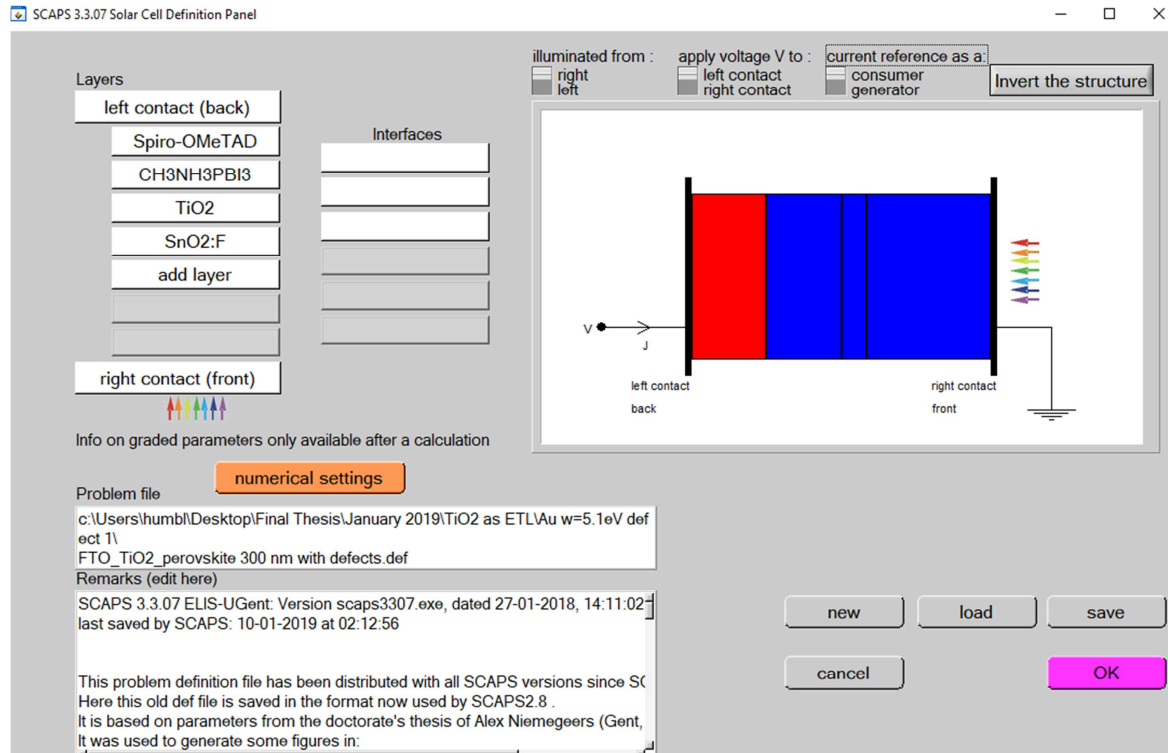


Figure 9. SCAPS-1D definition panel with PSC cell Layers name.

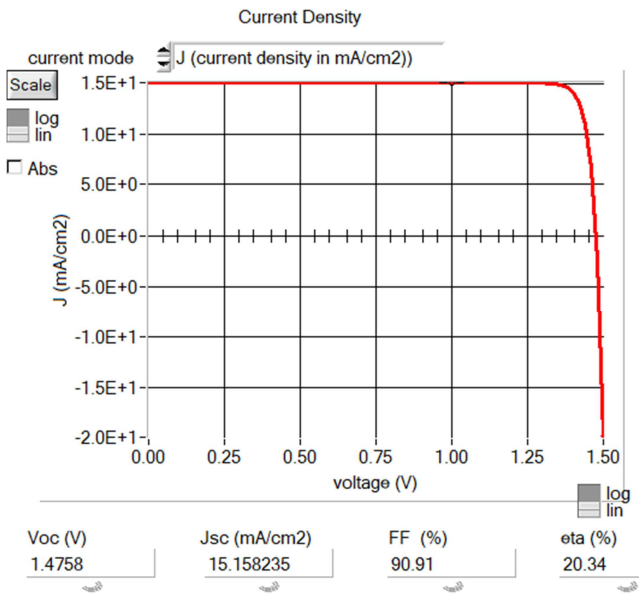


Figure 10. I-V characteristics curve of PSC with Au contacts.

5. Results and Discussion

In this study, we observed the thickness of the absorber layer, which has a very high absorption coefficient up to 105cm^{-1} . It is a very critical parameter that affects the PSC performance, and it is electrical properties such as (J_{sc} , V_{oc} , FF, and PCE), the short-circuit current density, the open-circuit voltage, Fill Factor and the power conversion efficiency, respectively. As the absorber thickness (vary from 50 to 600 nm). The default parameters for the other layers set,

as mentioned in Table 1. As shown in Figure 10, which shows the optimal cell performance around the thickness of 300nm for the active layer, and then decreases slightly. While V_{oc} increases to an optimal value at 200nm and then decreases afterward. For fill factor, it increases slowly when the thickness increases. The behavior of the efficiency is very similar to V_{oc} , increasing to an optimal value between 300nm and 400nm, and then decreases with the thickness increase. Another important property is the charge carriers in the perovskite active layer has a longer diffusion length than 300nm as the case of our model, where the electron and hole can reach their corresponding electrode before they recombine, which can enhance the efficiency [21].

Moreover, V_{oc} is defined by equation (8). More excess carrier's concentration gives a higher value of I_L , while I_0 stays at a low level because of not much recombination in the cell. This is the reason why V_{oc} increases for the first time. Fill Factor is defined as the ratio of the maximum generated power to the product of V_{oc} and I_{sc} when the thickness is less than 500nm. However, the PCE is increasing with the thickness increases to some degree. The internal power depletion is also increasing after 300 nm. While the thickness of more than 300 nm, we start noticing the decreasing effect on the PCE, which caused by more recombination happens because of the increasing number of traps and because more and more excess carriers cannot reach the electrodes. In this case, thicker absorber brings drops of V_{oc} and PCE. In this simulation, the performance of a solar cell is dominated by two factors, 1) How efficient is the active layer can absorb the photon. 2) How fast the charge carrier can move to the corresponding electrode [22, 23].

6. Conclusion

We employed the device simulator SCAPS 1D in the modeling of PSC. SCAPS-1D [24] simulator. The researchers widely use this program from around the world for modeling all type of solar cell. We have Au as a contact layer with a work function of 5.1eV, Spiro-Ometad, CH₃NH₃PBI₃ as an absorber layer with a different thickness between 50nm to 600nm, the results are shown in Table 2. Figure10 shows a 300nm thickness is an optimal thickness for the absorber with an efficiency of 20.34%, and TiO₂ as ETL.

Table 2. Shows the simulation results.

Thickness (nm)	Voc (V)	Jsc (mA/cm ²)	FF%	Efficiency %
50	1.4551	5.936405	89	7.7
100	1.471	9.708584	90	12.85
200	1.4772	13.804484	91	18.49
300	1.4758	15.158235	91	20.34
400	1.4726	15.042101	91	20.16
500	1.4689	14.159126	91	18.93
600	1.4652	12.912388	91	17.22

Acknowledgements

We would like to thank Dr. Marc Burgelman and his staff, at the University of Gent, Belgium, for the freely distributed SCAPS-1D simulator.

References

- [1] Frost JM, Butler KT, Brivio F, Hendon CH, Schilfgaarde MV, and Walsh A. Atomistic origin of high performance in. Hybrid halide perovskite solar cells. *Nano Lett.* 2014; 14: 2484-2590.
- [2] Baikie T, Fang YN, Kadro JM, Schreyer M, Wei FX, Mhaisalkar SG, Gratzel M, and White TJ "Synthesis And Crystal Chemistry Of The Hybrid Perovskite". <https://pubs.rsc.org/en/content/articlelanding/2013/ta/c3ta10518k> sensitized solar cell applications. *J. Mater. Chem. A.* 2013; 1: 5628–5641.
- [3] Stoumpos C, Malliakas CD, and Kanatzidis MG."Thermochromic Halide Perovskite Solar Cells [Nature materials." <https://www.nature.com/articles/s41563-017-0006-2013>; 52: 9019–9038.
- [4] "Synthesis And crystal Chemistry Of The Hybrid Perovskite"<https://pubs.rsc.org/en/content/articlelanding/2013/ta/c3ta10518k>.
- [5] Yin WJ, Yang JH, Kang J, Yan Y, and Wei SH. Halide perovskite materials for Solar cells: a theoretical review. *J. Mater. Chem. A.* 2014.
- [6] Walsh A, Watson GW. The origin of the stereochemically active Pb (II) lone Pair: DFT calculations on PbO and PbS. *Journal of Solid-State Chemistry.* 2005; 178: 1422–1428.
- [7] Walsh A, Payne DJ, Egdell RG, and Watson GW. Stereochemistry of post-Transition metal oxides: revision of the classical lone pair model. *Chem. Soc. Rev.* 2011; 40: 4455–446.
- [8] Keith T. Butler, Jarvis M. Frost, and Aron Walsh, Band alignment of the hybrid Halide perovskites CH₃NH₃PbCl₃, CH₃NH₃PbBr₃, and CH₃NH₃PbI₃. *Materials Horizons.* 2014; 2: 228-231.
- [9] Gray, D. E. American Institute of Physics Handbook, 3rd ed.; McGraw-Hill: New York, 1982.
- [10] Lide, D. R. CRC Handbook of Chemistry and Physics, 73rd ed; CRC Press: Boca Raton, FL, 1994.
- [11] Stranks, S. D.; Eperon, G. E.; Grancini, G.; Menelaou, C.; Alcocer, M. J. P.; Leijtens, T.; Herz, L. M.; Petrozza, A.; Snaith, H. J. Electron-Hole Diffusion Lengths Exceeding Micrometer in an Organometal Trihalide Perovskite Absorber. *Science* 2013, 342, 341–344.
- [12] Lee MM, Teuscher J, Miyasaka T, Murakami TN, and Snaith HJ. Efficient hybrid Solar cells based on meso-superstructure organometal halide perovskites. *Science.* 2012; 338: 643-647.
- [13] "Strong-Covalency-induced-Recombination-CentersIn..." <http://pubs.acs.org/doi/abs/10.1021/ja5079305>. 26May. 2019.
- [14] Liu F, Zhu J, Wei J, Li Y, Li M, Yang S, Zhang B, Yao J, and Dai S. Numerical simulation: Toward the design of high-efficiency planar perovskite solar cells. *Applied Physics Letters.* 2014; 104: 253508.
- [15] Walsh A, Watson GW. The origin of the stereochemically active Pb (II) lone pair: DFT calculations on PbO and PbS. *Journal of Solid-State chemistry.* 005; 178: 1422–1428.
- [16] Miyasaka T, Kojima A, Teshima K, and Shirai Y. Organometal halide perovskite As a visible- light sensitizer for photovoltaic cells. *Jour. of Americ. Chem. Soc.* 2009; 131: 6050-6051.
- [17] Walsh A, Payne DJ, Egdell RG, and Watson GW. Stereochemistry of post-transition metal oxides: revision of the classical lone pair model. *Chem. Soc. Rev.* 2011; 40: 4455–446.
- [18] G. Haacke, the New figure of merit for transparent conductors, *J. Appl. Phys.* 47.
- [19] Lee MM, Teuscher J, Miyasaka T, Murakami TN, and Snaith HJ. Efficient hybrid Solar cells based on meso-superstructure organometal halide perovskites. *Science.* 2012; 338: 643-647.
- [20] Jeon NJ, Lee HG, Kim YC, Seo J, Noh JH, Lee J, and Seok SI. O-Methoxy Substituents in Spiro-OMeTAD for Efficient inorganic-organic Hybrid Perovskite Solar Cells. *J. Am. Chem. Soc.* 2014; 136: 7837–7840.
- [21] Wang JT, Ball JM, Barea EM, Abate A, Alexander-Webber JA, Huang J, Saliba M, Mora-Sero I, Bisquert J, Snaith HJ, and Nicholas RJ. Low-temperature processed electron collection layers of graphene/TiO₂ nanocomposites in thin film perovskite solarCells. *Nano Letters.* 2014; 14: 724-730.
- [22] Wojciechowski K, Saliba M, Leijtens T, Abate A, and Snaith HJ. Sub-1500 C Processed meso-super structured perovskite solar cells with enhanced efficiency. *Energy Environ Sci.* 2014; 7: 1142-1147.
- [23] Jeon NJ, Lee HG, Kim YC, Seo J, Noh JH, Lee J, and Seok SI. O-Methoxy SubstituentsIn Spiro-OMeTAD for Efficient organic–OrganicHybrid perovskite Solar Cells. *J. Am. Chem. Soc.* 2014; 136: 7837–7840.

- [24] Zhou H, Chen Q, Li G, Luo S, Song T, Duan HS, Hong Z, Yu J, Liu Y, Yang Y. Interface Engineering of highly efficient perovskite solar cells. *Science*. 2014; 345: 542546.
- [25] Green MA, Emery K, Hishikawa Y, Warta W, and Dunlop ED. Solar cell efficiency tables (Version 45). *Prog. Photovolt: res. Appl.* 2015; 23: 1-9.